



Universiteit
Leiden
The Netherlands

Biochemistry in different phases of the migraine attack

Onderwater, G.L.J.

Citation

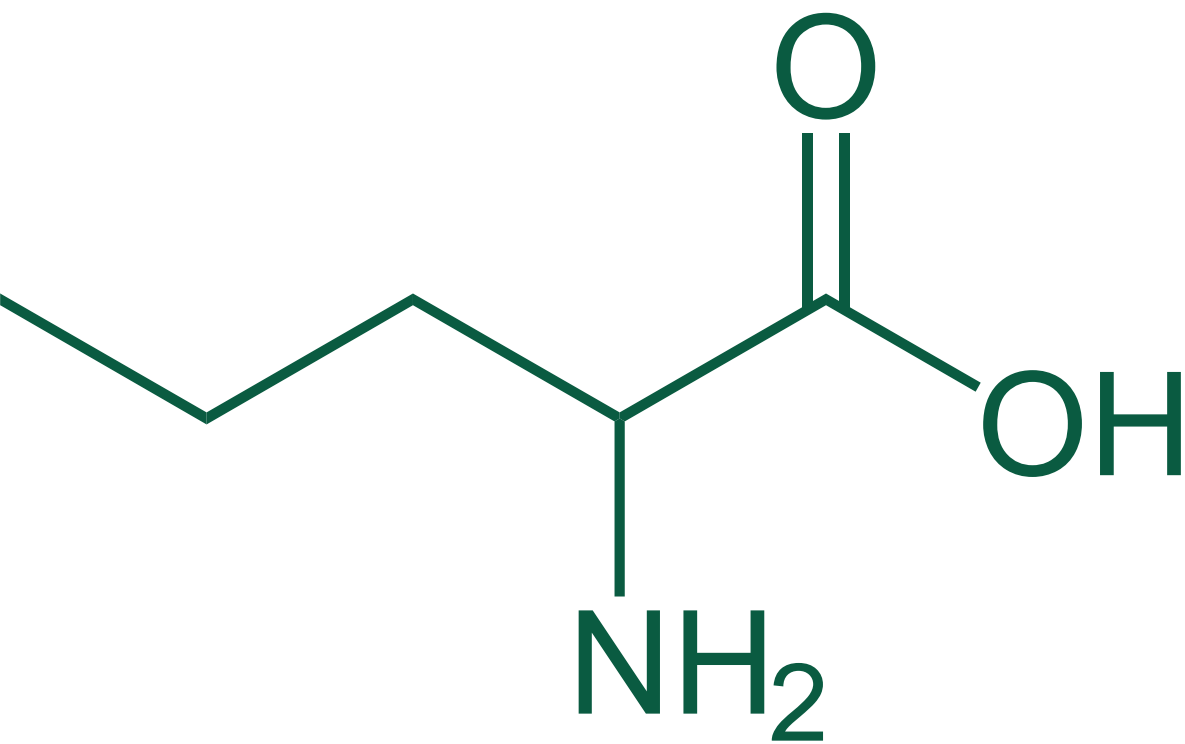
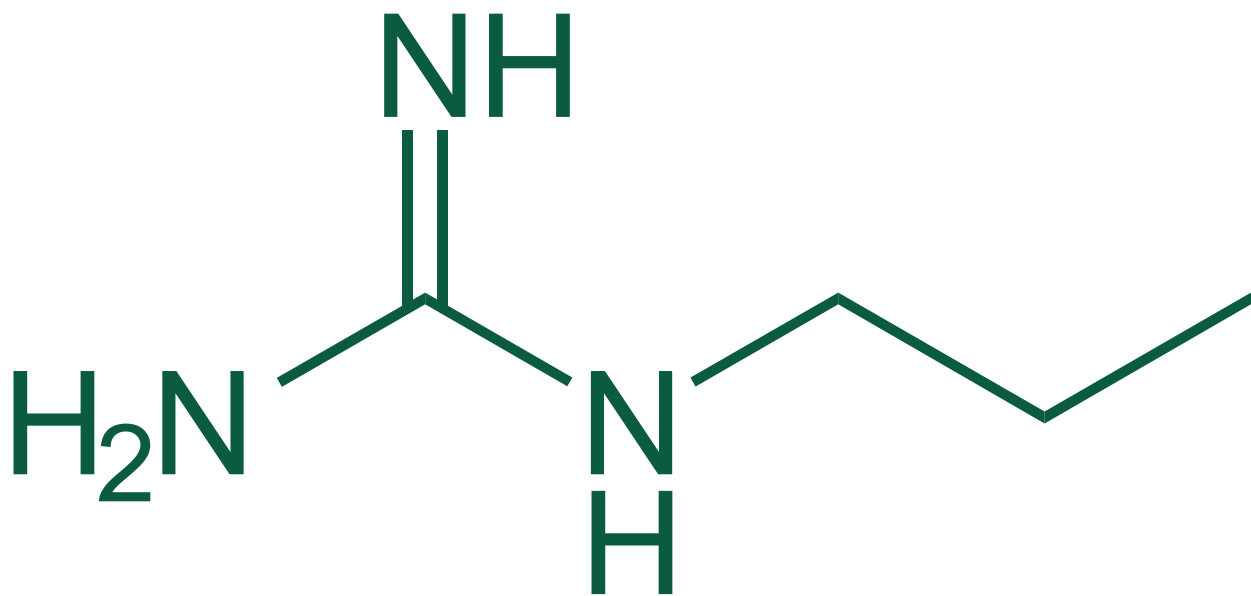
Onderwater, G. L. J. (2022, April 21). *Biochemistry in different phases of the migraine attack*. Retrieved from <https://hdl.handle.net/1887/3294052>

Version: Publisher's Version

License: [Licence agreement concerning inclusion of doctoral thesis in the Institutional Repository of the University of Leiden](#)

Downloaded from: <https://hdl.handle.net/1887/3294052>

Note: To cite this publication please use the final published version (if applicable).



Chapter 3

Cerebrospinal fluid and plasma amine profiles in migraine

G.L.J. Onderwater^{1*}, R.M. van Dongen^{1*}, A.C. Harms², R. Zielman¹,
W.P.J. van Oosterhout¹, J.B. van Klinken^{3,4}, J.J. Goeman⁵, G.M. Terwindt¹,
A.M.J.M. van den Maagdenberg^{1,4}, T. Hankemeier², M.D. Ferrari¹

¹Department of Neurology, Leiden University Medical Centre, Leiden, the Netherlands

²Division of Analytical Biosciences, Leiden Academic Centre for Drug Research, Leiden, the Netherlands

³Department of Human Genetics, Leiden University Medical Centre, Leiden, the Netherlands

⁴Department of Clinical Chemistry, Laboratory Genetic Metabolic Disease, Amsterdam University Medical Centre, Amsterdam, the Netherlands

⁵Department of Medical statistics and Bioinformatics, Leiden University Medical Centre, Leiden, the Netherlands

* Shared first authors

Abstract

Objective

Impaired cerebral and systemic amine metabolism have been implicated in migraine etiology. Direct evidence from CSF is, however, lacking. We aimed to assess individual amine levels, global amine profiles and amine pathways in CSF and plasma of interictal patients with migraine compared to healthy controls.

Methods

CSF and plasma were sampled between 08:30 am and 1:00 pm, at random from healthy volunteers ($n = 96$) and interictal patients with migraine ($n = 99$ with aura; $n = 98$ without aura). Groups were matched for age and sex. The study was approved by the Local Medical Ethics Committee. Individual amines ($n = 30$ in CSF; $n = 31$ in plasma), global amine profiles, and specific amine pathways were analyzed using an ultra-performance liquid chromatography mass spectrometry (UPLC-MS) platform that was validated for amine measurements.

Results

We analyzed $n = 197$ participants with migraine ($n = 99$ with aura; $n = 98$ without aura) and $n = 96$ healthy volunteers. Univariate analysis with Bonferroni correction indicated that CSF L-Arginine levels were reduced in migraine with aura (-10.4% ; $p < 0.001$) and without aura (-5.0% ; $p = 0.03$). FDR-corrected CSF L-Phenylalanine levels were also lower in both migraine with aura (6.9% ; $p = 0.011$) and without aura (-8.1% ; $p = 0.001$). The effect, however, failed to reach significance after Bonferroni correction ($p = 0.088$). Other amines did not differ. Multivariate analysis revealed that CSF global amine profiles were similar for both types of migraine ($p = 0.64$), but distinct from controls ($p = 0.009$). Global profile analyses were similar in plasma. Strongest associated pathways with migraine were related to L-Arginine metabolism.

Conclusions

Cerebral and systemic amine profiles are disrupted in migraine with and without aura. Reduced CSF L-Arginine and altered associated pathway analyses suggest dysfunction of nitric oxide signaling in migraine, which may serve as a potential preventive treatment target.

Introduction

Migraine is a common neurovascular brain disorder, characterized by disabling attacks of headache and associated symptoms for up to three days.^{1,2} In one third of patients, attacks may include aura.³ Women are affected three times more often.¹⁻³ Objective diagnostic biomarkers are lacking.² Median attack frequency is 1.5 per month and one quarter of patients experience weekly attacks.³ Genetic and non-genetic risk and susceptibility-modifying factors are involved.⁴ Although mechanisms for aura and headache are reasonably well understood^{5,6}, little is known about how attacks are initiated and why they continue recurring.^{1,4} This has hampered the development of causal therapy. Even the recently emerging CGRP inhibitors have limited effectiveness.^{6,7}

Unravelling migraine neurochemistry might help to elucidate its aetiology.^{4,8} Most biochemical studies in migraine have focused on blood and urine.^{5,9} While easier to collect, these biofluids mainly reflect systemic rather than cerebral changes.¹⁰ CSF might better reflect brain neurochemistry^{11,12}, but its sampling has been hampered by logistic and ethical issues.

Various amines such as glutamate, glutamine, GABA and serotonin have been implicated in migraine^{4,9,13}, but CSF studies were small and had methodological limitations. Controls were rarely matched for confounding factors such as sex, age, and diurnal and seasonal timing of sampling. They were also rarely truly healthy, which could potentially affect CSF composition. Lumbar punctures were usually done to exclude neurological disease in patients with neurological symptoms. In some studies, ictal CSF was only compared with interictal CSF, without healthy controls. These reports focused on the pathophysiology of the attack, rather than on pathogenetic mechanisms of “the disease migraine” (i.e. why does someone experience recurring migraines?). Details of the measurement methods and their validation were often limited.⁹ Finally, studies only reported on single or just a few molecules, rather than on multiple substances, simultaneously measured in both CSF and plasma and allowing for unbiased analysis of global profiles and pathways.

To identify abnormalities in amine levels, global profiles, and pathways, we assessed 31 amines in CSF and plasma of 96 healthy volunteers and 197 interictal migraineurs with (n = 99) or without (n = 98) aura. Groups were matched for age, sex, and timing of sampling.

Methods

Study design and participants

We enrolled patients with migraine with or without aura² and healthy controls who were

group-matched for sex and age (by adhering to 5-year age strata). Migraineurs did not use acute migraine drugs on more than 8 days per month. CSF and plasma were collected interictally when patients had been attack-free for ≥ 3 days. Sampling occurred between April 2008 and May 2016. Healthy volunteers had no obvious signs or symptoms of a disease and had no history of headache (except for infrequent tension-type headaches) or other pain syndromes. They also did not have first-degree relatives with migraine or trigeminal autonomic cephalgia. Participants did not have a severe psychiatric disorder, nor a history of oncological disease, or a contra-indication for lumbar puncture (signs and symptoms of increased intracranial pressure, local skin infection, or a coagulopathy including use of anti-coagulant drugs or platelet-inhibitors). The study was conducted according to the criteria of the Declaration of Helsinki and approved by the Leiden University Medical Centre institutional ethics committee. All participants provided written informed consent prior to participation and received financial compensation according to standard fees for participation in similar studies.

Sample collection

Sampling occurred between 08:30 a.m. and 1:00 p.m., randomly for patients and controls, to mitigate diurnal and seasonal variation differences. Participants refrained from eating or drinking, apart from water, for at least 8 hours prior to sampling. After standard neurological examination, CSF was sampled by lumbar puncture between the L3/L4, L4/L5, or L5/S1 interspace. Intracranial pressure was measured, and 3.0 mL CSF was sampled for routine diagnostics (cell count, glucose and total protein levels). Next, 3.8 mL of CSF was sampled directly in a 15-mL polypropylene falcon tube pre-chilled on ice and centrifuged at 4°C for 5 minutes (2,000 rpm, 747 g). The supernatant was transferred into a new chilled 15-mL polypropylene falcon tube, inverted several times, and divided in 0.5 mL aliquots (1.8-mL cryotubes) that already contained 1.0 mL of cold EtOH. Cryotubes were inverted several times to mix CSF and EtOH. Samples were placed on dry ice within 30 minutes of sampling and stored at -80°C within 60 minutes. Blood was collected from the median cubital vein in EDTA plasma tubes, immediately after lumbar puncture, and centrifuged at 21°C for 20 minutes (2,000 rpm, 622 g). The supernatant was transferred to a new 15-mL polypropylene falcon tube, inverted several times, and divided in 0.5 mL aliquots (1.0-mL Nunc™ cryotubes). Plasma samples were stored at -80°C within 60 minutes from sampling. All CSF and plasma samples remained at -80°C until sample preparation, no extra freeze-thaw cycles were allowed. See figure S1 for detailed information on sample processing. To monitor complications, participants were followed for three days, or longer if necessary.

Amine measurements

Amines were measured with an ultra-performance liquid chromatography mass spectrometry (UPLC-MS) method specifically developed for amine profiling.¹⁴ Samples

were randomized across five CSF batches and five plasma batches. All batches included calibration lines, blanks and quality control samples. Blanks were used to subtract background levels from study samples. Quality control samples were analyzed every 10 samples and were used to monitor data quality and to correct for instrument response.¹⁵ For the analysis of CSF, 30 μL of CSF/EtOH sample was spiked with an internal standard solution. For the analysis of plasma, 5 μL of starting material was used. For the analysis of amino acids, $^{13}\text{C}^{15}\text{N}$ -labeled analogues were used.¹⁴ For other amines, the closest-eluting internal standard was added. The target list is included as table S1. After spiking, proteins were precipitated by the addition of MeOH and the mixture was vortexed for 10 s and centrifuged (9,400 g for 10 min at 10°C). The supernatant was transferred to a new eppendorf tube and taken to dryness in a Speedvac. The residue was reconstituted in borate buffer (pH 8.5) with 6-aminoquinolyl-N-hydroxysuccinimidyl carbamate reagent. Next, vials were transferred to an autosampler tray and cooled to 4°C until injection. Some 1.0 μL of the reaction mixture was injected into the UPLC-MS system. Chromatographic separation was achieved by an ACQUITY UPLC System (Waters) on an Accq-Tag Ultra column (Waters) with a flow of 0.7 mL/min over a 11-min gradient. The UPLC was coupled to electrospray ionization on a triple quadrupole mass spectrometer (Qtrap 6500, AB SCIEX, Nieuwekerk aan den IJssel, the Netherlands). Analytes were detected in the positive ion mode and monitored in Multiple Reaction Monitoring (MRM) using nominal mass resolution. Acquired data were evaluated using MultiQuant Software for Quantitative Analysis (Version 3.0.2, AB SCIEX), by integration of assigned MRM peaks and normalization using internal standards.

Statistical analysis

Amine concentrations were first corrected based on quality control samples.¹⁵ Only metabolites with relative standard deviations of quality controls below 15% were included in further analyses. Outlier detection was performed using principal component analysis (PCA) with a 99% confidence interval (figure S2). Log-transformed concentrations were used for further statistical analyses.

To detect univariate metabolite differences, ANCOVA analysis was performed with age and sex as covariates. Bonferroni was used for multiple testing correction, separately for CSF (30 tests) and plasma (31 tests). Additionally, we analyzed the data using the less conservative False Discovery Rate (FDR). For significant metabolites ($p < 0.05$ after multiple testing correction) *post hoc* comparisons were tested according to Shaffer's method.¹⁶

To detect multivariate differences in global metabolite profile or amine pathways, the Global Test approach¹⁷ was used (separately for CSF and plasma). First, global amine profiles of the three groups were compared with age and sex as covariates. Second, pathways were tested. We used MetaboAnalyst to obtain KEGG (Kyoto Encyclopedia

of Genes and Genomes) identifiers from the 31 amines and subsequently downloaded KEGG metabolite set pathway definitions from ConsensusPathDB (07-11-2018).

To ensure that metabolite sets represented coherent pathways we computed a metabolic interaction network of the 31 amines from the human Genome-Scale Metabolic Model (GSMM) HMR 2.0.¹⁸ To avoid overgeneralized conclusions (for example, stating that pathway 'X' is altered whereas only 3/12 of the metabolites of that pathway were measured) we introduced the criterium that all measured metabolites in the pathway must be connected with each other, either directly or within two reaction steps. This resulted in several pathways. Only pathways with at least three measured amines were included; we considered pathways of two amines too small. See supplementary methods for further details on this metabolic network approach.

To test whether these pathways differed between the three groups we used the Global Test function with the pathways as subsets and age and sex as covariates. Bonferroni was used to correct for the final number of pathways ($n = 6$). To visualize the generated amine network and examine the reaction paths between connected metabolites, we developed an interactive HTML/JavaScript document (e-methods).

Finally, to determine whether amine profiles could predict diagnosis a logistic regression model was developed. Migraine diagnosis was set as dependent variable and amines, age and sex were used as predictors. Overfitting of the model was prevented using L2 ridge penalisation.¹⁹ Predictions resulted from cross validation. Statistical analyses were done with R (version 3.4.1), R packages global test (version 5.30.0) and penalized (version 0.9-50) and SPSS (version 23). Two-sided hypothesis testing was used.

Data availability

The data that support the findings of this study are available from the corresponding author, upon reasonable request.

Results

Study population

We included 96 healthy volunteers and 197 patients with migraine, 99 with aura and 98 without aura. Five healthy controls turned out to have a first-degree relative with migraine but were kept in the study because CSF of healthy volunteers is so precious and separate analysis of these five controls did not yield aberrant results. In one patient with migraine with aura we were unable to collect plasma. Additionally, two outliers were excluded from further data analysis (figure S2). There were no differences in clinical

characteristics between the final study groups (table 1) except for a higher monthly attack frequency (2.8 ± 2.6) in migraine without aura versus migraine with aura (2.1 ± 1.9 ; $p = 0.026$). In total 92 (31.4%) participants developed post-dural puncture headache (table S2) of which eighteen required a blood patch.

Table 1. Clinical characteristics of participants

	Healthy controls	Migraine with aura	Migraine without aura	P-value
Number of participants^a	95	98	98	
Subject characteristics				
Females	56 (58.9)	65 (66.3)	60 (61.2)	0.553 ^c
Age, years	38.8 (14.5)	41.7 (13.6)	42.0 (12.9)	0.170 ^d
BMI	23.7 (2.8)	24.0 (2.7)	23.6 (2.5)	0.602 ^e
Smoking	20 (21.1)	13 (13.3)	13 (13.3)	0.245 ^e
Overnight fasting				
Fasting time, hours	11.6 (2.4)	11.7 (1.7)	11.9 (1.6)	0.105 ^d
Migraine characteristics				
Migraine frequency, attacks/month	-	2.1 (1.9)	2.8 (2.6)	0.026^f
Headache days, days/month	0.3 (0.7)	5.2 (4.2)	6.0 (4.9)	<0.001^d
Migraine <3 days after LP				0.168 ^a
No	-	85 (86.7)	79 (80.6)	
Yes	-	11 (11.2)	18 (18.4)	
Unknown	-	2 (2.0)	1 (1.0)	
Medication use				
Triptan	-	58 (59.6)	71 (72.4)	0.050 ^e
Prophylactic medication	-	17 (17.3)	17 (17.3)	1.000 ^e
B-blocker	-	11 (11.2)	9 (9.2)	0.637 ^e
Antiepileptic drug	-	4 (4.1)	4 (4.1)	1.000 ^g
Ace-inhibitors	-	1 (1.0)	1 (1.0)	1.000 ^g
Angiotensin II receptor antagonist	-	2 (2.0)	1 (1.0)	1.000 ^g
Sampling characteristics				
Opening pressure in mmH ₂ O	19.1 (4.4)	18.8 (4.0)	18.0 (4.7)	0.250 ^e
CSF characteristics				
Erythrocytes, count/3μL	154 (934)	2,299 (20,682)	130 (505)	0.509 ^d
Leukocytes, count/3μL	6.0 (6.0)	22.0 (89.0)	5.0 (7.0)	0.587 ^d
Protein concentration, g/L	0.35 (0.13)	0.36 (0.25)	0.35 (0.10)	0.702 ^d
Glucose, mmol/L	3.2 (0.3)	3.2 (0.3)	3.1 (0.2)	0.738 ^e
Post-dural puncture headache^b				
Cases	31 (32.3)	24 (24.2)	37 (37.8)	0.121
Duration, days	5.35 (3.34)	4.52 (2.8)	4.15 (2.33)	0.206
Blood patch	5 (5.2)	7 (7.0)	6 (6.1)	0.953

^aShown for CSF after exclusion of two outliers (see Methods), ^bfor these variables all participants who received an LP were included. ^cChi-square test. ^dKruskal-Wallis Test. ^eOne-way ANOVA. ^fMann-Whitney test. ^gFisher's Exact Test. $p < 0.05$ are depicted in bold. LP=lumbar puncture. Data are n, mean (SD), or n (%), unless otherwise stated.

Univariate results

In total 30 amines were reliably detected in CSF, and 31 in plasma. In CSF, L-Arginine levels were different between the three groups (table 2; $p = 0.042$ after Bonferroni correction). *Post hoc* analysis showed 10.4% lower levels in migraine with aura ($p < 0.001$) and 5.0% lower levels in migraine without aura ($p = 0.027$) versus controls without difference between migraine subtypes ($p = 0.153$) (figure 1). Since L-Arginine is potentially related to cardiovascular status²⁰, we repeated the analysis after exclusion of participants with possible cardiovascular comorbidities ($n = 12$) or antihypertensive medication for migraine prevention ($n = 20$), but differences remained significant (table S3). Participants who developed a migraine attack ≤ 3 days after sampling (and thus potentially were in a preictal phase), did not show different results (figure S3). The ability of L-Arginine to predict migraine was modest with an area under the curve of 0.657 for migraine with aura and 0.560 for migraine without aura (figure S4).

None of the other metabolites in CSF differed significantly after Bonferroni correction (table 2). Using FDR correction, CSF L-Phenylalanine also differed; concentrations were reduced in migraine with aura (-6.9%; $p = 0.011$) and without aura (-8.1%; $p = 0.001$; figure S5).

In plasma there were no metabolite differences after correction for multiple comparisons (table 3 and figure S6).

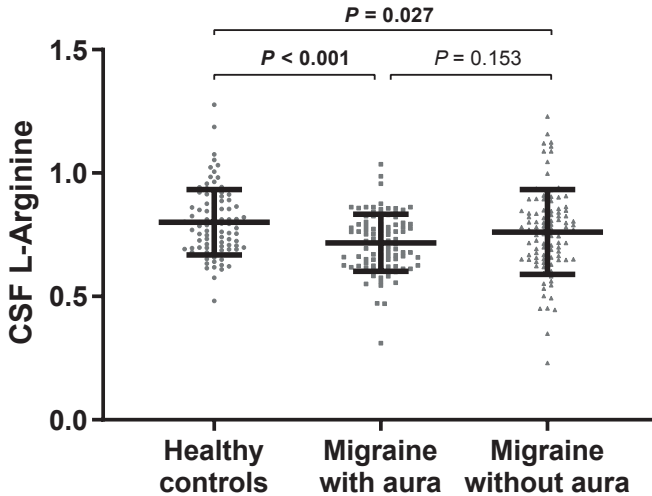


Figure 1. CSF L-Arginine levels in participants with migraine and healthy controls. Individual CSF L-Arginine levels are plotted (dots) with group means \pm SD (bars). Data are adjusted for age. p -values are from *post-hoc* analysis after ANCOVA.

Table 2. Univariate analysis results in CSF

Metabolite	Sex	Age	Diagnosis	Bonferroni	FDR
	<i>P</i> -value	<i>P</i> -value	<i>P</i> -value		
L-Arginine	0.0002	0.0000	0.0014	0.0422	0.0422
L-Phenylalanine	0.0078	0.0000	0.0029	0.0881	0.0441
L-Asparagine	0.2080	0.0000	0.0101	0.3022	0.0767
Ethanolamine	0.1481	0.5817	0.0102	0.3069	0.0767
L-Methionine	0.0001	0.0000	0.0149	0.4482	0.0896
L-Glutamine	0.0000	0.0000	0.0200	0.5987	0.0998
Taurine	0.0000	0.0000	0.0510	1.0000	0.2519
Ornithine	0.0010	0.0000	0.0598	1.0000	0.2503
L-Homoserine	0.7510	0.0204	0.0860	1.0000	0.5000
L-Tyrosine	0.0169	0.0000	0.0871	1.0000	0.2335
L-Tryptophan	0.8322	0.2757	0.0909	1.0000	0.2585
L-2-aminoadipic-acid	0.8585	0.0004	0.0997	1.0000	0.4966
L-Isoleucine	0.0000	0.0000	0.1012	1.0000	0.7089
Gamma-aminobutyric acid	0.0120	0.0000	0.1172	1.0000	0.8132
L-Leucine	0.0000	0.0000	0.1251	1.0000	0.5119
Citrulline	0.0000	0.0000	0.1343	1.0000	0.2335
L-4-hydroxy-proline	0.0047	0.0224	0.1465	1.0000	0.2335
N6-N6-N6-Trimethyl-Lysine	0.0416	0.0026	0.2104	1.0000	0.2503
L-Lysine	0.0357	0.0000	0.2514	1.0000	0.3970
Putrescine	0.0000	0.0001	0.2720	1.0000	0.6620
L-Valine	0.0000	0.0000	0.3495	1.0000	0.8864
L-Alanine	0.0506	0.0000	0.3642	1.0000	0.6935
Glycine	0.1652	0.0000	0.3834	1.0000	0.2335
L-Histidine	0.4174	0.2717	0.4095	1.0000	0.2335
L-Proline	0.0082	0.0000	0.5517	1.0000	0.4966
3-Methoxytyrosine	0.0126	0.0006	0.5957	1.0000	0.3507
L-Threonine	0.5953	0.0102	0.6242	1.0000	0.2242
L-Alpha-aminobutyric acid	0.1929	0.0000	0.6616	1.0000	0.4081
L-Glutamic acid	0.1449	0.7921	0.7861	1.0000	0.2186
L-Serine	0.0053	0.0328	0.8864	1.0000	0.6874

p-values depicted are from an analysis of covariance (ANCOVA) between the study groups (diagnosis) with age and sex as covariates. Metabolites are ranked by *p*-value of diagnosis. FDR=false discovery rate correction. In bold: $p < 0.05$ after multiple testing correction.

Table 3. Univariate analysis results in plasma

Metabolite	Sex	Age	Diagnosis	Bonferroni	FDR
	<i>p</i> -value	<i>p</i> -value	<i>p</i> -value		
Citrulline	0.0000	0.0000	0.0063	0.1965	0.0857
L-Arginine	0.0001	0.0570	0.0079	0.2439	0.0857
L-4-hydroxy-proline	0.0000	0.0008	0.0083	0.2572	0.0857
O-Phosphoethanolamine	0.5608	0.1047	0.0435	1.0000	0.3370
Taurine	0.0830	0.8983	0.0592	1.0000	0.3673
Ethanolamine	0.0000	0.0571	0.0820	1.0000	0.4234
N6-N6-N6-Trimethyl-Lysine	0.0000	0.1537	0.1298	1.0000	0.4982
L-Tryptophan	0.0000	0.0021	0.1580	1.0000	0.4982
L-Lysine	0.0086	0.0262	0.1631	1.0000	0.4982
L-Isoleucine	0.0000	0.1417	0.1679	1.0000	0.4982

Table 3. Continued.

Metabolite	Sex	Age	Diagnosis	Bonferroni	FDR
	<i>p</i> -value	<i>p</i> -value	<i>p</i> -value		
L-Glutamic acid	0.0000	0.6273	0.2162	1.0000	0.4982
L-Leucine	0.0000	0.9974	0.2188	1.0000	0.4982
L-Glutamine	0.0000	0.0003	0.2240	1.0000	0.4982
3-Methoxytyrosine	0.1295	0.0971	0.2348	1.0000	0.4982
L-Histidine	0.0625	0.0018	0.2547	1.0000	0.4982
L-2-aminoadipic acid	0.0000	0.0001	0.2592	1.0000	0.4982
L-Methionine	0.0000	0.0439	0.3018	1.0000	0.4982
L-Phenylalanine	0.0000	0.0868	0.3228	1.0000	0.4982
L-Proline	0.0000	0.8231	0.3337	1.0000	0.4982
L-Homoserine	0.0151	0.2065	0.3469	1.0000	0.4982
L-Valine	0.0000	0.0774	0.3510	1.0000	0.4982
L-Asparagine	0.3512	0.1308	0.3536	1.0000	0.4982
L-Alanine	0.0001	0.2295	0.4013	1.0000	0.5408
Putrescine	0.0115	0.1437	0.4306	1.0000	0.5562
L-Tyrosine	0.0000	0.0000	0.5789	1.0000	0.6961
L-Threonine	0.3757	0.2104	0.5839	1.0000	0.6961
L-Serine	0.6010	0.7000	0.7065	1.0000	0.8112
Gamma-aminobutyric acid	0.9494	0.4597	0.8354	1.0000	0.9249
Glycine	0.0983	0.0000	0.8879	1.0000	0.9492
L-Alpha-aminobutyric acid	0.1532	0.0008	0.9282	1.0000	0.9591
Ornithine	0.0000	0.0000	0.9817	1.0000	0.9817

p-values depicted are from an analysis of covariance (ANCOVA) between the study groups (diagnosis) with age and sex as covariates. Metabolites are ranked by *p*-value of diagnosis. FDR = false discovery rate correction. In bold: $p < 0.05$ after multiple testing correction.

Multivariate results

In CSF, global metabolite profiles differed between groups ($p = 0.035$). While there were no differences between migraine subtypes ($p = 0.640$), profiles for migraine with aura ($p = 0.029$), migraine without aura ($p = 0.020$), and all migraine participants combined ($p = 0.009$) differed from those in controls (figure 2). Again, the ability to predict migraine was modest, with an area under the curve of 0.67 for migraine with aura and 0.63 for migraine without aura (figure S7).

Plasma, results were similar to those in CSF. Profiles differed between groups ($p = 0.021$). While there were no differences between migraine subtypes ($p = 0.275$), profiles for migraine with aura ($p = 0.028$), migraine without aura ($p = 0.018$) and all migraine ($p = 0.011$) differed from those in controls. The area under the curve of the prediction model was 0.61 for migraine with aura and 0.57 for migraine without aura (figure S8).

Pathways present in our metabolite set are visualized in figure 3. In CSF, the pathway “arginine biosynthesis” was significantly associated with migraine with aura (figure 4). The “arginine/proline metabolism” pathway showed the strongest association with migraine

without aura, but this was not multiple testing resistant. In plasma, strongest associated pathways were “arginine biosynthesis” with migraine with aura and “arginine/proline metabolism” with migraine without aura (figure 4), but only significant before multiple testing correction. Exclusion of L-Arginine, to study the effect of other metabolites in these pathways, showed similar results (table S4).

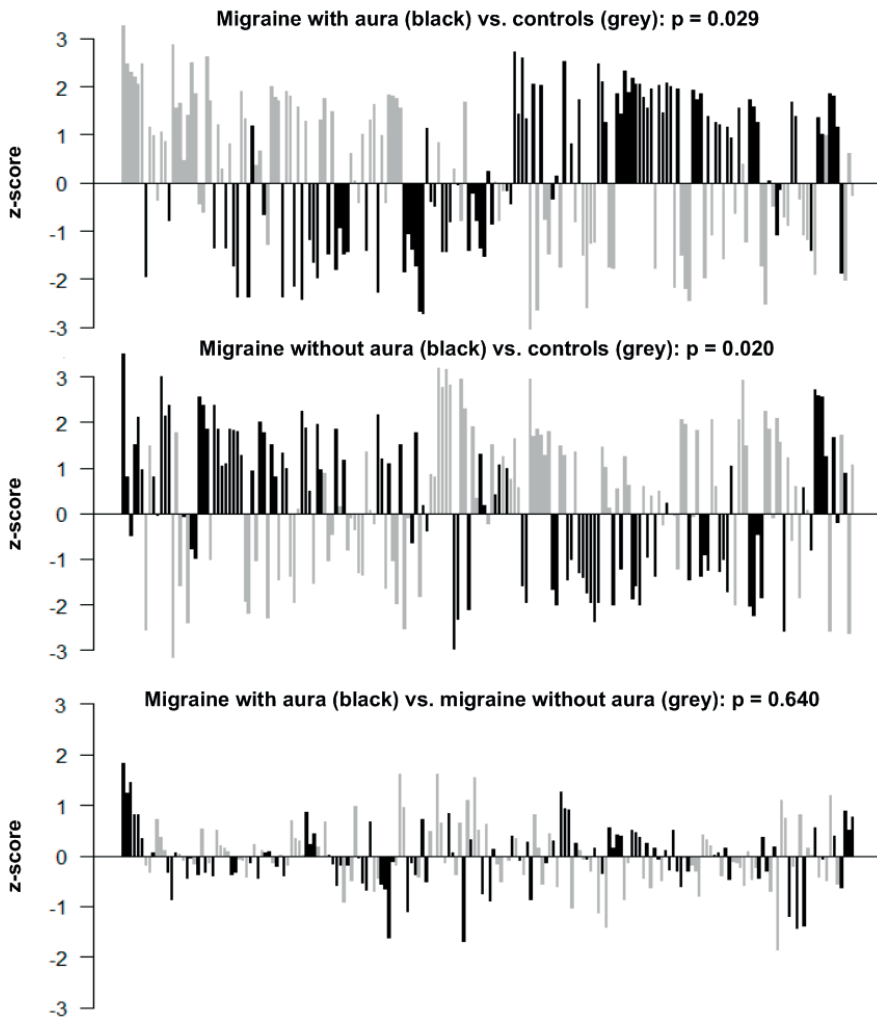


Figure 2. Subjects plot of global test with all amines in CSF. P -values are from the global test. For each participant (bars) the z-score is plotted. A positive z-score indicates the metabolite profile of the participant matches with the profile of his or her group. A negative z-score indicates the profile of the participant matches better with the profile of the other group. The number of the z-score reflects the strength of the match. For the comparisons migraine with aura versus controls (upper panel) and migraine without aura versus controls (middle panel), there are relatively more participants with high positive z-scores than for the comparison migraine with aura versus migraine without aura (lower panel).

Discussion

We analyzed individual amines, global amine profiles and amine pathways in the CSF and plasma of a uniquely large study population of interictal patients with migraine with or without aura and healthy volunteers. CSF L-Arginine levels were 10.4% reduced in migraine with aura and 5.0% in migraine without aura. Global CSF and plasma amine profiles were similar in migraineurs with and without aura but differed from those of healthy volunteers. Pathway analysis results also point toward L-Arginine metabolism in migraine with aura.

L-Arginine has never been measured in CSF of migraineurs.^{9,21} Previous studies in serum, plasma, platelets, saliva, and urine have produced inconsistent findings across and within biofluids.^{22–25} The compound is unevenly distributed in the CNS, with the greatest pool in astrocytes, less so in neuronal tissue, and absent in oligodendrocytes.²⁶ L-Arginine is involved in endocrine activity, immune system modulation, regulation of vascular tone, and CNS peptide and protein production.²⁶ In the CNS, metabolism of L-Arginine is closely connected with the metabolism of citrulline and ornithine, that can be synthesized and degraded into each other. Citrulline and ornithine, however, were not abnormal in our study (figure S9). Nonetheless, pathway analysis revealed that although the results seem primarily driven by L-Arginine, there was still an association between migraine and ‘arginine biosynthesis’ when excluding L-Arginine (although not multiple testing resistant). This suggests that other metabolites from these pathways, including citrulline and ornithine, could still be involved. Catabolism of L-Arginine leads to formation of agmatine, guanidonoacetic acid (ultimately forming creatine) or urea²⁶; all metabolites that could not be measured on our platform.

L-Arginine is also linked to the formation of nitric oxide, which has been implicated in migraine pathophysiology.²⁶ Glyceryl trinitrate, a nitric oxide donor, can provoke migraine-like attacks in migraineurs but not in non-migraineurs.²⁷ Nitric oxide elevates the levels of cyclic guanosine monophosphate (cGMP), an important second messenger which is believed to play a central role in migraine pathophysiology, since it is the common pathway of not only glyceryl trinitrate but also other migraine provocation models.²⁷ Nitric oxide production is catalyzed by nitric oxide synthase (NOS) for which L-Arginine serves as the only available nitrogen-containing substrate.²⁶ There are three isoforms of NOS: endothelial (e), neuronal (n), and inducible (i) NOS.²⁶ The observed lower CSF L-Arginine concentrations might therefore reflect overactivity of NOS. A non-selective NOS inhibitor was suggested to be effective in spontaneous migraine attacks^{28,29}, while specific iNOS inhibitors failed and trials with combinations of a nNOS blocker and a triptan showed conflicting results.^{27,29,30} Still, our findings offer support that nitric oxide signaling is involved in migraine pathophysiology, also outside attacks. The nitric oxide pathway could

be more upstream in the migraine cascade than the CGRP pathway, since CGRP levels were found to be elevated in migraine attacks provoked by nitric oxide.³¹ Furthermore, premonitory symptoms (symptoms which precede migraine headache) are frequently reported in glyceryl trinitrate provoked attacks^{32,33}, while being rare in CGRP-provoked attacks.³⁴ Therefore, L-Arginine might be a more upstream target than CGRP.

Using the less conservative FDR correction, L-Phenylalanine CSF levels were lower in both migraine subtypes. Humans cannot synthesize L-Phenylalanine *de novo*.²⁶ Therefore, the concentrations are fully dependent on dietary intake. Although participants were fasting, long-term dietary differences cannot be excluded and therefore findings must be interpreted with caution. We observed no difference in tyrosine, the hydrolyzation product of L-Phenylalanine but tyrosine also has a dietary component.²⁶

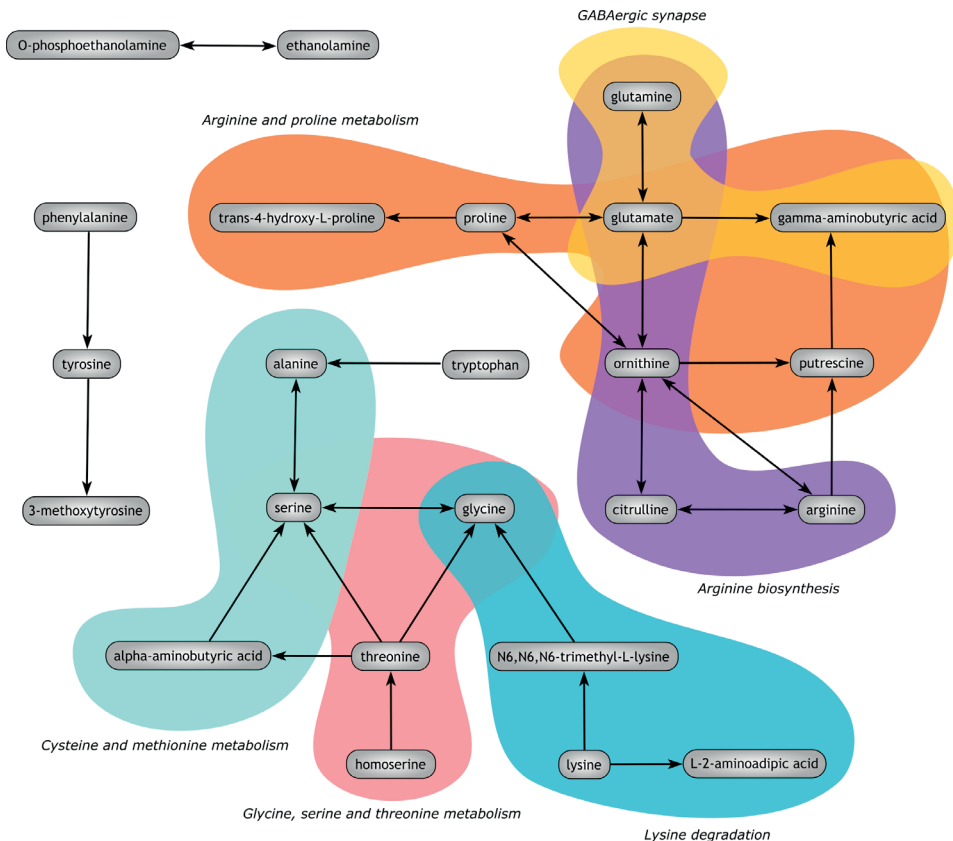


Figure 3. Metabolic network. Visualization of the generated GSMM network. Only metabolites that lie within two reaction steps of each other are visualized (thereby excluding L-asparagine, L-methionine, taurine, L-isoleucine, L-leucine, L-valine and L-histidine). Colors indicate KEGG pathways that were tested using the global test approach

Our study has several strengths. Study groups were considerably larger than in other studies⁹ and matched for major confounding factors such as sex, age, and timing of sampling. Control CSF was as normal as possibly could. Unlike in other studies⁹, controls were truly healthy. CSF was not collected because of neurological symptoms. Controls were also not to have first degree relatives with migraine, to minimize the genetic risk of still developing migraine later on.^{4,35} Finally, where other studies only measured single or a just few molecules, and either in CSF or plasma⁹, we on the contrary, simultaneously assessed multiple amines in both CSF and plasma, using a dedicated and validated UPLC-MS platform, allowing for additional profile and pathway analyses.

We used a network-based pathway analysis approach to investigate which pathways could underlie the altered CSF and plasma amine profiles of migraine patients. We found this approach especially useful for metabolomics data where coverage of the pathway definitions is low compared to e.g. transcriptomics data. Consequently, it is only possible to make assertions about part of the pathway, that is not the full KEGG pathway. If studied metabolites only reside on extreme ends of the pathway diagram or are only connected through enzymatic steps that do not occur in humans, it would be incorrect to draw statistical conclusions of the full KEGG pathway. Therefore, we used the described filtering step. Combining classic pathway definitions with knowledge about how the measured amines are connected through human metabolism, we were able to define metabolite sets for pathway analysis that are more accurate and relevant from a biochemical point of view.

Ideally, we should have replicated our findings in an independent study population, but collecting a second, sufficiently large, matched sample of CSF and plasma from migraineurs and healthy volunteers is logistically challenging, expensive, and time consuming. Moreover, to assess the specificity of our findings, we should also have investigated other non-migraine headaches, e.g. tension-type headache. Furthermore, extended pathway coverage by measuring additional amines and other pathways is needed to improve our understanding of migraine biochemistry. However, we prioritized reliable quantification above a broader range of detection. Another limitation is the cross-sectional nature of our study. Repeated sampling, ideally across the entire migraine attack cycle, would have afforded more detailed insight into migraine biochemistry, but seems ethically impossible. Finally, the effects in our study were modest and overlap, hence the observed differences are unlikely to be useful as diagnostic tests.

Extensive amine profiling in CSF and plasma shows that brain and systemic amine profiles are altered in interictal patients with migraine, similarly in migraineurs with or without aura. Reduced CSF L-Arginine and altered associated pathway analyses suggest dysfunction of nitric oxide signaling in migraine, which may serve as a potential preventive treatment target.

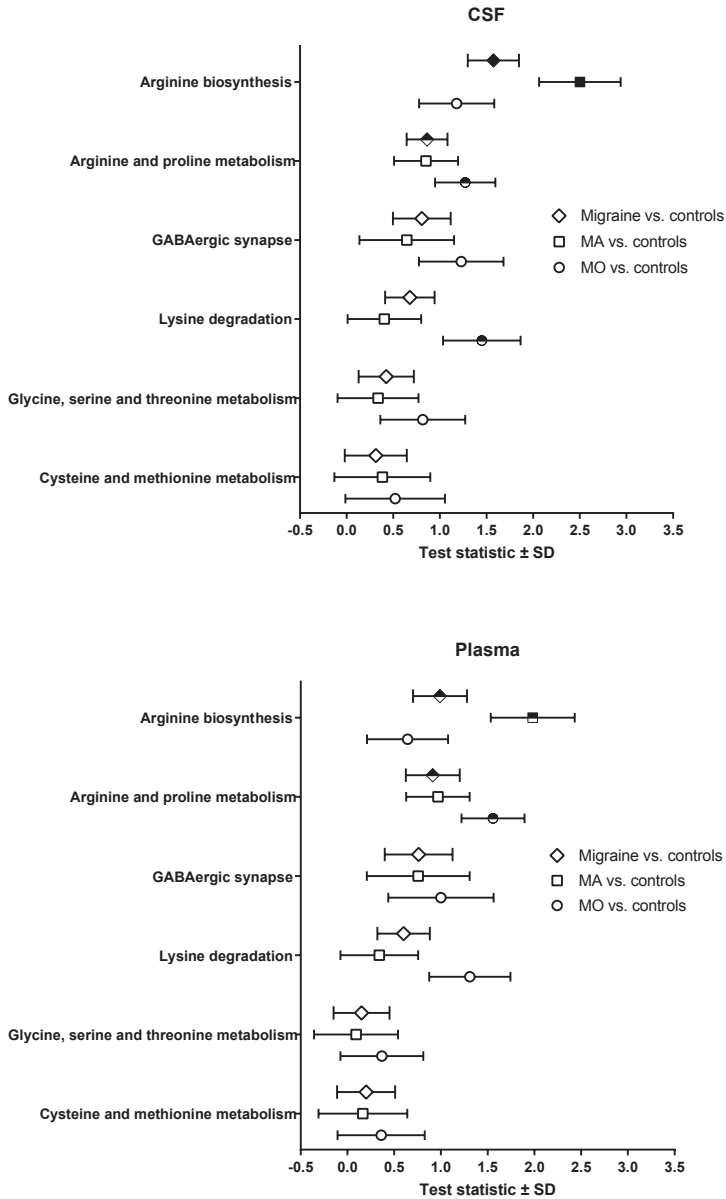


Figure 4. Pathway analysis results. Results from the global test approach on pathways. The global test is aimed at associations between sets of connected metabolites and disease status and does not test the direction of the association. i.e. whether sets of metabolites are up- or down-regulated. Therefore, there is not a mean difference to plot and one can only visualize the test statistic and corresponding standard deviation (SD). MO=migraine without aura, MA=migraine with aura, Migraine=both subtypes combined, full black symbol= $p < 0.05$ after multiple testing correction with Bonferroni, half black symbol= $p < 0.05$ before multiple testing correction.

Study funding

This work was supported by the Netherlands Organization for Scientific Research (VICI grant no. 918.56.601 and Spinoza 2009 to MDF), the Netherlands Organization for Health Research and Development (Clinical Fellowship grant no. 90700217 and Vidi grant no. 917-11-31 to GMT), and European Community (EC) funded FP7-EUROHEADPAIN (grant no. 602633 to MDF and AMJMvdM).

Acknowledgement

We greatly acknowledge all study participants, the medical students who assisted with recruitment of participants, physicians Floor Bakels, Nadine Pelzer, Leopoldine Wilbrink and Anne van der Plas for sample collection, and Erik van Zwet and Slavik Koval for their advice on the applied statistics.

References

1. GBD 2016 Disease and Injury Incidence and Prevalence Collaborators. Global, regional, and national incidence, prevalence, and years lived with disability for 328 diseases and injuries for 195 countries, 1990–2016: a systematic analysis for the Global Burden of Disease Study 2016. *Lancet* **390**, 1211–1259 (2017).
2. Headache Classification Committee of the International Headache Society (IHS). The International Classification of Headache Disorders, 3rd edition. *Cephalalgia* **1**, 1–211 (2018).
3. Launer, L. J., Terwindt, G. M. & Ferrari, M. D. The prevalence and characteristics of migraine in a population-based cohort: the GEM study. *Neurology* **53**, 537–542 (1999).
4. Ferrari, M. D., Klever, R. R., Terwindt, G. M., Ayata, C. & van den Maagdenberg, A. M. J. M. Migraine pathophysiology: lessons from mouse models and human genetics. *Lancet Neurol.* **14**, 65–80 (2015).
5. Goadsby, P. J. *et al.* Pathophysiology of Migraine – A disorder of sensory processing. *Physiol Rev* **97**, 553–622 (2017).
6. Edvinsson, L., Haanes, K. A., Warfvinge, K. & Krause, D. N. CGRP as the target of new migraine therapies – successful translation from bench to clinic. *Nat. Rev. Neurol.* **14**, 338–350 (2018).
7. Charles, A. & Pozo-Rosich, P. Targeting calcitonin gene-related peptide: a new era in migraine therapy. *Lancet* **394**, 1765–1774 (2019).
8. Stankewitz, A. & May, A. The phenomenon of changes in cortical excitability in migraine is not migraine-specific – A unifying thesis. *Pain* **145**, 14–19 (2009).
9. van Dongen, R. M. *et al.* Migraine biomarkers in cerebrospinal fluid: A systematic review and meta-analysis. *Cephalalgia* **37**, 49–63 (2017).
10. Wishart, D. S. *et al.* The human cerebrospinal fluid metabolome. *J. Chromatogr. B. Analyt. Technol. Biomed. Life Sci.* **871**, 164–173 (2008).
11. Brown, P. D., Davies, S. L., Speake, T. & Millar, I. D. Molecular mechanisms of cerebrospinal fluid production. *Neuroscience* **129**, 957–970 (2004).
12. Deisenhammer, F., Teunissen, C. E. & Tumani, H. *Cerebrospinal Fluid in Neurologic Disorders, Volume 146 1st Edition.* (2017). doi:10.1016/B978-0-12-804279-3.00016-2
13. Humphrey, P. P. A. *et al.* Serotonin and Migraine. *Ann. N. Y. Acad. Sci.* **600**, 587–598 (1990).
14. Noga, M. J. *et al.* Strategies to assess and optimize stability of endogenous amines during cerebrospinal fluid sampling. *Metabolomics* **14**, 44 (2018).
15. Van Der Kloet, F. M., Bobeldijk, I., Verheij, E. R. & Jellema, R. H. Analytical error reduction using single point calibration for accurate and precise metabolomic phenotyping. *J. Proteome Res.* **8**, 5132–5141 (2009).
16. Shaffer, J. P. Modified Sequentially Rejective Multiple Test Procedures. *J. Am. Stat. Assoc.* **81**, 826–831 (1986).
17. Hendrickx, D. M., Hoefsloot, H. C. J., Hendriks, M. M. W. B., Canelas, A. B. & Smilde, A. K. Global test for metabolic pathway differences between conditions. *Anal. Chim. Acta* **719**, 8–15 (2012).
18. Mardinoglu, A. *et al.* Genome-scale metabolic modelling of hepatocytes reveals serine deficiency in patients with non-alcoholic fatty liver disease. *Nat. Commun.* **5**, 3083 (2014).
19. Goeman, J. J. L1 penalized estimation in the Cox proportional hazards model. *Biometrical J.* **52**, 70–84 (2010).
20. Moss, M. B., Siqueira, M. A., Mann, G. E., Brunini, T. M. & Mendes-Ribeiro, A. C. Platelet aggregation in arterial hypertension: Is there a nitric oxide-urea connection? *Clin. Exp. Pharmacol. Physiol.* **37**, 167–172 (2010).

21. Zielman, R. *et al.* Metabolomic changes in CSF of migraine patients measured with 1 H-NMR spectroscopy. *Mol. BioSyst.* **12**, 3674–3682 (2016).
22. Sjaastad, O., Gjesdahl, P. & Gjessing, L. R. Amino acids in urine in spontaneous migraine attacks. *Eur. J. Neurol.* **7**, 137–145 (1972).
23. Rajda, C. *et al.* Amino acids in the saliva of patients with migraine. *Headache* **39**, 644–649 (1999).
24. D'andrea, G. *et al.* Decreased collagen-induced platelet aggregation and increased platelet arginine levels in migraine: A possible link with the NO pathway. *Cephalalgia* **14**, 352–356 (1994).
25. Reyhani, A. *et al.* High asymmetric dimethylarginine, symmetric dimethylarginine and L-arginine levels in migraine patients. *Neurol. Sci.* **38**, 1287–1291 (2017).
26. Oja, S. S., Schousboe, A. & Saransaari, P. *Handbook of neurochemistry and molecular neurobiology.* (2007). doi:10.1007/978-0-387-30373-4
27. Ashina, M., Hansen, J. M., á Dunga, B. O. & Olesen, J. Human models of migraine — short-term pain for long-term gain. *Nat. Rev. Neurol.* **13**, 713–724 (2017).
28. Lassen, L. H., Ashina, M., Christiansen, I., Ulrich, V. & Olesen, J. Nitric oxide synthase inhibition in migraine. *Lancet* **349**, 401–402 (1997).
29. Goadsby, P. J. Bench to bedside advances in the 21st century for primary headache disorders: Migraine treatments for migraine patients. *Brain* **139**, 2571–2577 (2016).
30. Macone, A. E. & Perloff, M. D. Triptans and migraine: advances in use, administration, formulation, and development. *Expert Opin. Pharmacother.* **18**, 387–397 (2017).
31. Juhasz, G. *et al.* NO-induced migraine attack: Strong increase in plasma calcitonin gene-related peptide (CGRP) concentration and negative correlation with platelet serotonin release. *Pain* **106**, 461–470 (2003).
32. Afridi, S. K., Kaube, H. & Goadsby, P. J. Glyceryl trinitrate triggers premonitory symptoms in migraineurs. *Pain* **110**, 675–80 (2004).
33. Onderwater, G. L. J., Dool, J., Ferrari, M. D. & Terwindt, G. M. Premonitory symptoms in glyceryl trinitrate triggered migraine attacks: a case-control study. *Pain* **161**, 2058–2067 (2020).
34. Guo, S., Vollesen, A. L. H., Olesen, J. & Ashina, M. Premonitory and nonheadache symptoms induced by CGRP and PACAP38 in patients with migraine. *Pain* **157**, 2773–2781 (2016).
35. Russell, M. B. & Olesen, J. Increased familial risk and evidence of genetic factor in migraine. *BMJ* **311**, 541–4 (1995).

Supplementary data

Supplementary Methods. Detailed procedures.

Sample collection

See figure S1 for an illustration of the sample collection.

Genome-Scale Metabolic Model analysis

We used the human Genome-Scale Metabolic Model (GSMM) HMR2.0¹ to determine the biochemical interconversions between the amines that were measured on our metabolomics platform. All computations described in this section were performed in MATLAB. To facilitate the mapping of metabolomics data to the GSMM, we enriched the model with compound synonyms and external identifiers from the ChEBI database (downloaded 28-6-2018)², where ChEBI identifiers and synonyms of conjugate acids and bases were also included. Of the 31 amines that were measured, all mapped to the GSMM.

Biochemical interactions between metabolites were determined by converting the GSMM into a weighted directed graph where nodes represent metabolites and edges represent reactions. Subsequently all reaction paths between the amines that involved one or two reaction steps were determined using a generic path finding algorithm that was developed *in house*. To ensure the reaction paths represented relevant biochemical conversions, a set of 10 hub metabolites (H₂O, H, CO₂, O₂, Pi, PPI, PPPi, CoA, THF and SAM) was excluded from the path finding procedure. In addition, the GSMM-based graph was defined in such a way that half-reactions involving the transfer of electrons, amino groups and other chemical moieties were decoupled from the main reaction. That is, in the reaction $\text{NADH} + \text{pyruvate} \rightleftharpoons \text{NAD}^+ + \text{lactate}$, only NADH and NAD⁺ are linked in the graph and pyruvate and lactate are linked. Likewise, in the reaction $\text{glutamate} + \text{pyruvate} \rightleftharpoons \text{AKG} + \text{alanine}$, only glutamate and AKG are linked and pyruvate and alanine are linked. Finally, reactions that produced a metabolite that occurred with low frequency in the model were assumed to be tightly coupled to that metabolite and were therefore given a weight of zero. Specifically, for metabolites that were produced by only one or two reactions - where iso-reactions were counted as a single reaction - the corresponding reactions were given a weight of zero. Also transporter reactions that transferred compounds over the cellular membranes were given a weight of zero.

To facilitate the inspection of the network analysis results, an interactive HTML/JavaScript document was written that imported and visualized the GSMM-based amine network and the reaction paths corresponding to the network links. Reaction information was enriched by importing tissue-specific gene expression from the Human Protein Atlas (HPA)³ and Genotype-Tissue Expression (GTEx)⁴ project. Pathway analysis resulted in a

two larger connected networks of respectively 9 and 10 amines (Fig. 3) and two smaller networks of only ethanolamine and o-Phospho-ethanolamine and of phenylalanine, tyrosine and 3-methoxytyrosine. Finally, we introduced the criterium that all measured metabolites in the pathway must be connected with each other, either directly or within two reaction steps. For seven of the amines (L-asparagine, L-methionine, taurine, L-isoleucine, L-leucine, L-valine and L-histidine) no link was found with another amine within two reaction steps; consequently, these amines were left out of the network visualization.

Network-based pathway analysis

In order to perform pathway analysis on the amine data, we used MetaboAnalyst⁵ to obtain KEGG identifiers from the 31 amines and subsequently downloaded KEGG metabolite set pathway definitions from ConsensusPathDB (07-11-2018). When inspecting the KEGG pathway diagrams it became clear that most KEGG pathways were not covered in a coherent fashion by our platform. Specifically, we encountered two types of issues: (1) some amines that mapped to a single pathway were distant from one another in the corresponding KEGG pathway diagram and we did not measure enough intermediate metabolites to consider the pathway covered and (2) some amines were mapped to a pathway due to enzymatic conversions that do not occur in humans.

To resolve these issues, we chose to use the GSMM-based amine network as filter for the KEGG metabolite sets. Each pathway set of amines was mapped to the GSMM-based network and subsequently we looked up whether those amines represented a connected subgraph, i.e. a graph where each node of a pathway is reachable within one or multiple steps by any other node of the pathway. Then a new list of pathway metabolite sets was generated representing the identified connected subgraphs for each of the traditional KEGG metabolite set pathway definitions. Connected subgraphs of one or two nodes only were eliminated from the list. The resulting list of pathway metabolite sets consisted of 10 independent pathways, where there were three metabolite sets that overlapped with other sets.

- Cysteine and methionine metabolism
- Glycine, serine and threonine metabolism
- Lysine degradation
- GABAergic synapse (same set definition as alanine, aspartate and glutamate metabolism)
- Arginine and proline metabolism (Glutathione metabolism is a subset of this pathway)
- Arginine biosynthesis
- Aminoacyl-tRNA biosynthesis (same set definition as Protein digestion and

absorption)

- Central carbon metabolism in cancer
- Mineral absorption
- ABC transporters

After inspection of the new list of metabolite sets we decided to exclude the last four pathways because they involved unspecific biological processes that were not relevant for this study.

References Supplementary Methods

1. Mardinoglu A, Agren R, Kampf C, Asplund A, Uhlen M, Nielsen J. Genome-scale metabolic modelling of hepatocytes reveals serine deficiency in patients with non-alcoholic fatty liver disease. *Nat Commun.* 2014;5:3083.
2. Hastings J, Owen G, Dekker A, et al. ChEBI in 2016 : Improved services and an expanding collection of metabolites. *Nucleic Acids Res.* 2016;44:1214-1219. doi:10.1093/nar/gkv1031
3. Uhlén M, Fagerberg L, Hallström BM, et al. Tissue-based map of the human proteome. *Science (80-).* 2015;347(6220):1260419. doi:10.1126/science.1260419
4. The GTEx Consortium. The Genotype-Tissue Expression (GTEx) project. *Nat Genet.* 2013;45(6):580-585. doi:10.1038/ng.2653.The
5. Xia J, Sinelnikov I V., Han B, Wishart DS. MetaboAnalyst 3.0-making metabolomics more meaningful. *Nucleic Acids Res.* 2015;43(W1):W251-W257. doi:10.1093/nar/gkv380

Table S1. Target list

Target molecule	Internal Standard	RSD_QC	RSD_QC
		CSF	Plasma
Beta-Alanine ^a	Beta-Alanine-D4	Very low signal	Very low signal
Citrulline	L-Threonine-13C15N	4%	3%
Ethanolamine	L-Aspartic acid-13C15N	3%	3%
Gamma-aminobutyric acid	L-Alpha-aminobutyric acid-D6	7%	10%
Glycine	Glycine-13C15N	3%	2%
L-2-aminoadipic acid	L-Alpha-aminobutyric acid-D6	3%	4%
L-4-hydroxy-proline	L-Asparagine-13C15N	15%	3%
L-Alanine	L-Alanine-13C15N	3%	2%
L-Alpha-aminobutyric acid	L-Alpha-aminobutyric acid-D6	3%	3%
L-Arginine	L-Arginine-13C15N	3%	4%
L-Asparagine	L-Asparagine-13C15N	2%	2%
L-Glutamic acid	L-Glutamic acid-13C15N	5%	3%
L-Glutamine	L-Glutamine-13C15N	2%	3%
L-Histidine	L-Asparagine-13C15N	15%	3%
L-Homoserine	Glycine-13C15N	5%	6%
L-Isoleucine	L-Isoleucine-13C15N	2%	2%
L-Leucine	L-Leucine-13C15N	2%	1%
L-Lysine	L-Lysine-13C15N	3%	2%
L-Methionine	L-Methionine-13C15N	2%	3%
L-Phenylalanine	L-Phenylalanine-13C15N	2%	1%
L-Proline	L-Alpha-aminobutyric acid-D6	2%	3%
L-Serine	L-Serine-13C15N	3%	3%
L-Threonine	L-Threonine-13C15N	2%	2%
L-Tryptophan	L-Tryptophan-13C15N	2%	1%
L-Tyrosine	L-Tyrosine-13C15N	3%	2%
L-Valine	L-Valine-13C15N	2%	2%
N6,N6,N6-Trimethyl-L-lysine	Beta-Alanine-D4	5%	5%
O-Phosphoethanolamine ^b	1-Methylhistidine-D3	3%	3%
Ornithine	Ornithine-D6	4%	3%
Putrescine	L-Alpha-aminobutyric acid-D6	4%	14%
Taurine	L-Asparagine-13C15N	3%	3%
3-Methoxytyrosine	2-(4-hydroxy-3-methoxyphenyl) ethyl-amine-1,1,2,2-D4	9%	5%
Glycylglycine ^c	1-Methylhistidine-D3	33%	10%
N-Methylhistidine ^d	1-Methylhistidine-D3	20%	4%

The final data set used for further statistical analysis consisting of 30 metabolites for CSF and 31 metabolites for plasma. ^aBeta-alanine was excluded from further statistical analysis because no reliable signals were observed. ^bO-Phosphoethanolamine was excluded from further statistical analysis because of the batch problem described below (CSF only; since plasma levels were normal we did analyse the plasma data). ^cGlycylglycine was excluded from further statistical analysis because RSD_QC values were >15%. ^dN-Methylhistidine was excluded from further statistical analysis because RSD_QC values were >15%. Abbreviation: RSD_QC=relative standard deviation of quality control samples.

Table S2. Postdural puncture headache based on needle type

Needle type	No postdural puncture headache	Postdural puncture headache
	(n = 201)	(n = 92)
Traumatic 20 gauge (n, %)	125 (65.1)	67 (34.9)
Atraumatic 20 gauge (n, %)	26 (66.7)	13 (33.3)
Atraumatic 22 gauge (n, %)	50 (83.3)	10 (16.7)
Atraumatic 24 gauge (n, %)	0 (0.0)	2 (100.0)

Table S3. Sensitivity analyses CSF L-Arginine

Statistical model	Migraine with aura vs. controls	Migraine without aura vs. controls
	P-value	P-value
Model 1	0.0003	0.0266
Model 2	0.0003	0.0378
Model 3	0.0008	0.0452
Model 4	0.0009	0.0530

Model 1: All participants, age and gender as covariates.

Model 2: Excluding n=12 participants with minor cardiovascular comorbidity: diabetes (n=1), hypercholesterolemia in medical history or use of lipid-lowering drugs (n=3), hypertension in medical history or use of antihypertensive drugs for hypertension (n=7) and aorta valve stenosis (n=1).

Model 3: Excluding n=12 participants minor cardiovascular comorbidity (described above) and excluding n=20 migraineurs who used antihypertensive drugs as migraine prophylaxis.

Model 4: Same as model 3 except smoking was added as additional covariate because after exclusion of participants relatively more controls smoked (25.3%) than migraine patients (14.7% for migraine with aura and 14.7% for migraine without aura). There were no differences in mean BMI (\pm SD): controls 23.63 (\pm 2.76), migraine with aura 23.87 (\pm 2.72) and migraine without aura 23.53 (\pm 2.57).

Table S4. Pathway results excluding L-Arginine

CSF	Comparison	P-value including	P-value excluding
		L-Arginine	L-Arginine
Arginine biosynthesis	Migraine vs. controls	$P = 0.0041$	$P = 0.0182$
	Migraine with aura vs. controls	$P = 0.0035$	$P = 0.0340$
	Migraine without aura vs. controls	$P = 0.0713$	$P = 0.1120$
Arginine and proline metabolism	Migraine vs. controls	$P = 0.0309$	$P = 0.0723$
	Migraine with aura vs. controls	$P = 0.1511$	$P = 0.4310$
	Migraine without aura vs. controls	$P = 0.0321$	$P = 0.0417$
Plasma	Comparison	P-value including	P-value excluding
Arginine biosynthesis	Migraine vs. controls	$P = 0.0380$	$P = 0.0615$
	Migraine with aura vs. controls	$P = 0.0139$	$P = 0.0484$
	Migraine without aura vs. controls	$P = 0.2951$	$P = 0.2320$
Arginine and proline metabolism	Migraine vs. controls	$P = 0.0251$	$P = 0.0376$
	Migraine with aura vs. controls	$P = 0.1003$	$P = 0.2956$
	Migraine without aura vs. controls	$P = 0.0136$	$P = 0.0105$

Pathway analysis was repeated for two pathways ('Arginine biosynthesis' and 'Arginine and proline metabolism') excluding L-Arginine to study the effect of the other metabolites in these pathways. See figure 3 in the main article for pathway visualization. p-values shown here were not corrected for multiple testing.

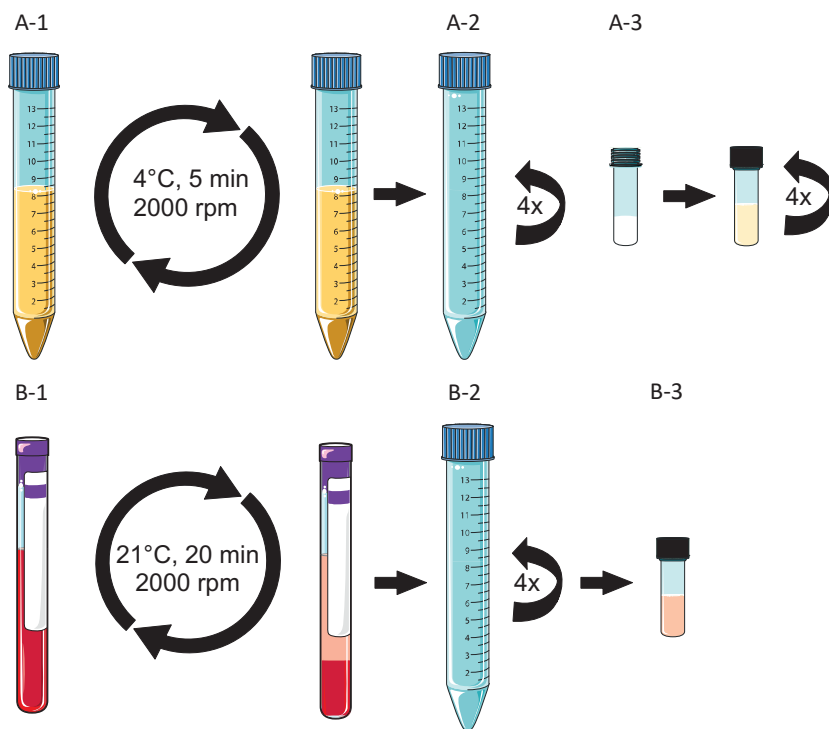


Figure S1. Sampling protocol. (A1-A3) CSF: Polypropylene tube (A-1; 15 mL, Cat. No. 188 271, Greiner Bio-One, Alphen aan den Rijn, the Netherlands) is kept in a cup with crushed ice until directly prior to CSF collection. Tube A-1 is filled to 3.8 mL, after sampling the filled tube is put back in the cup with crushed ice. The A-1 tube is then placed in a pre-cooled centrifuge and centrifuged for 5 minutes at 2,000 rpm, 647 g at 4°C. After centrifugation A-1 is placed on crushed ice, and the supernatant is removed and transferred to tube A-2. Polypropylene tube (A-2), containing the supernatant is gently inverted four times in order redistribute all compounds present in the CSF. Following swerving, while working on ice, 0.5 mL supernatant is transferred to a cryotube (A-3; 1.8 mL, Nunc™; Cat. No. 368632, Sigma-Aldrich, Zwijndrecht, the Netherlands) prefilled with 1 mL EtOH (Prod. No.:8098, ethanol absolute, J.T.Baker, Arnhem, the Netherlands) kept on dry ice. Cryotubes filled with CSF are gently inverted four times and put directly in the container with dry ice. After preparation all cryotubes are stored at -80°C. (B1-B3) Plasma: Blood is collected in Ethylenediaminetetraacetic acid (EDTA) plasma tubes (B-1; 10 mL, Cat. No. 366643, BD Medical, Vianen, the Netherlands) and kept at room temperature. The filled EDTA plasma tube is then placed in a centrifuge and centrifuged for 20 minutes at 2,000 rpm, 622 g at 21°C. After centrifugation B-1 is kept at room temperature, and the supernatant is removed and transferred to tube B-2. Polypropylene tube (B-2), containing the supernatant is gently inverted four times in order redistribute all compounds present in plasma. Following swerving, 0.5 mL supernatant is transferred to a cryotube (B-3; 1.0 mL, Nunc™ cryotubes; Cat. No. 366656, Sigma-Aldrich, Zwijndrecht, the Netherlands). Cryotubes filled with plasma are put directly after preparation in a -80°C freezer for storage.

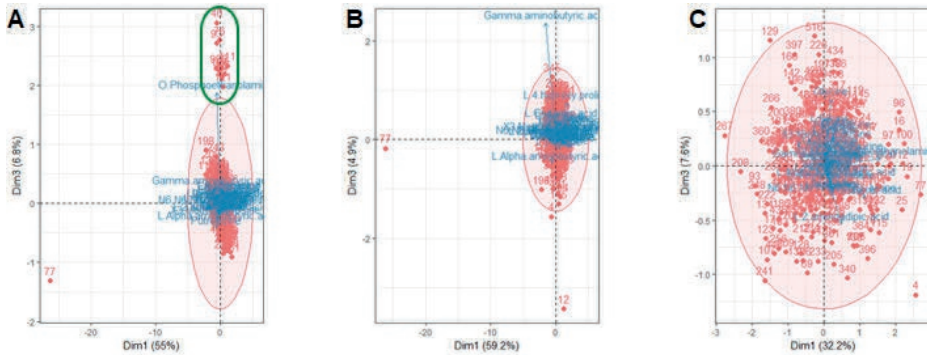


Figure S2. Outlier detection using principal component analysis. (A) CSF profile. Score plot from principal component analysis (red circle indicates the 99% C.I.). Thirteen out of 14 outlying samples had high levels of o-phosphoethanolamine (green circle); all 13 were measured in the same batch. Therefore, CSF o-phosphoethanolamine was excluded from further analysis. Sample 77 was an outlier because unexpected machine shutdown occurred during injection of the CSF and therefore excluded from statistical analysis (CSF only). Plasma levels of o-phosphoethanolamine from these participants were normal (data not shown) and therefore not excluded from further analysis. (B) CSF profile excluding o-phosphoethanolamine. Score plot from principal component analysis (red circle indicates the 99% C.I.). Sample 77 was an outlier because unexpected machine shutdown occurred during injection of the CSF and therefore excluded from statistical analysis (of CSF only). Sample 4 was retrospectively not a healthy control (percutaneous coronary interventions, diabetes) and therefore excluded from statistical analysis (of both CSF and plasma). Sample 12 had low gamma-aminobutyric acid levels but there were no further analytical abnormalities or clinical reasons to exclude the sample from statistical analysis. (C) Plasma profile. Score plot from principal component analysis (red circle indicates the 99% C.I.). Sample 4 was retrospectively not a healthy control (percutaneous coronary interventions, diabetes) and therefore excluded from statistical analysis (of both CSF and plasma). The other outliers were not excluded.

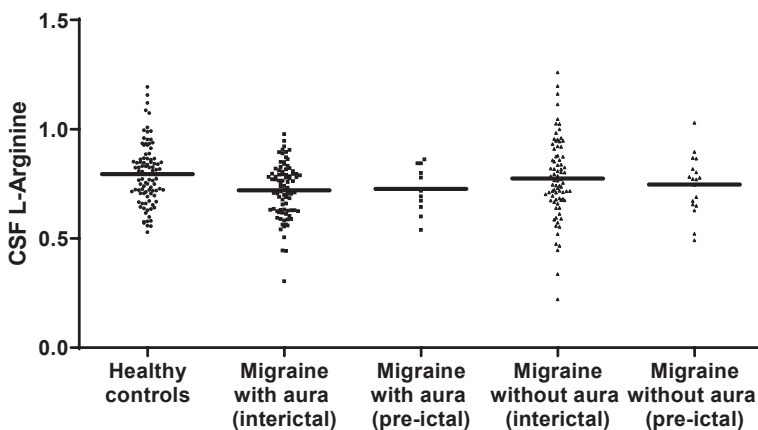


Figure S3. CSF L-Arginine levels separate for (potentially) pre-ictal patients and interictal patients. Individual CSF L-Arginine levels are plotted (dots) with group means (bar).

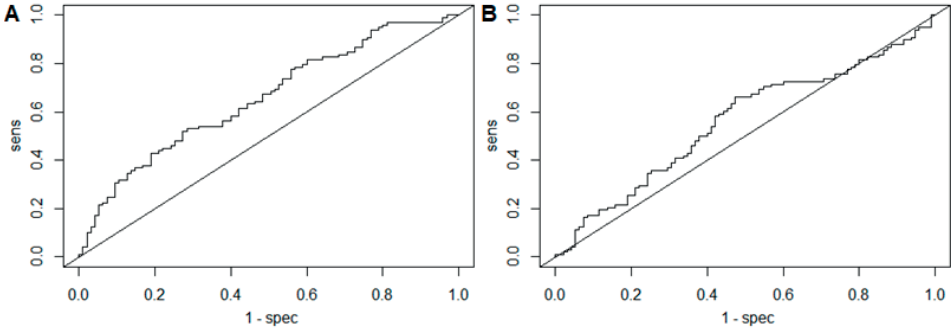


Figure S4. Receiver operator characteristics (ROC) curves for CSF L-Arginine. (A) Migraine with aura versus controls: area under the curve (AUC)=0.657. (B) Migraine without aura versus controls: area under the curve (AUC)=0.560, sens=sensitivity, spec=specificity.

3

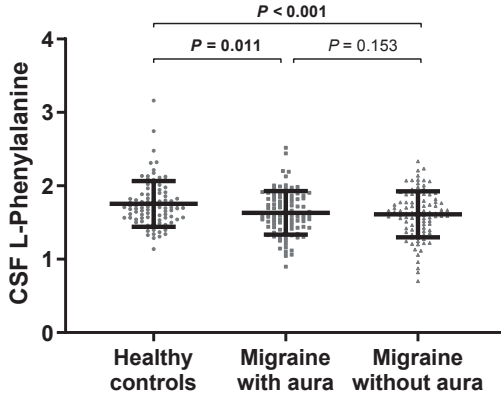


Figure S5. CSF L-Phenylalanine levels in participants with migraine and healthy controls. Individual levels are plotted (dots) with group means \pm SD (bars). Data and p-values are adjusted for age. P-values are from post-hoc analysis after ANCOVA.

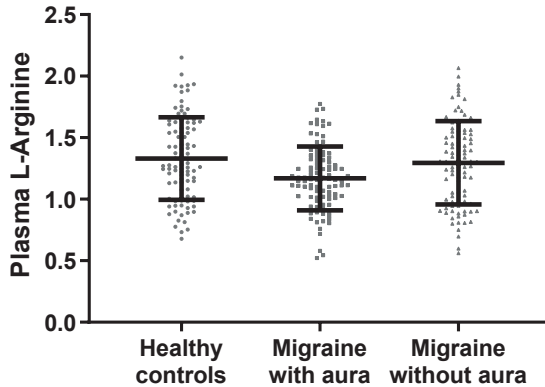


Figure S6. Plasma L-Arginine levels in participants with migraine and healthy controls. Individual levels are plotted (dots) with group means \pm SD (bars). Data are adjusted for age.

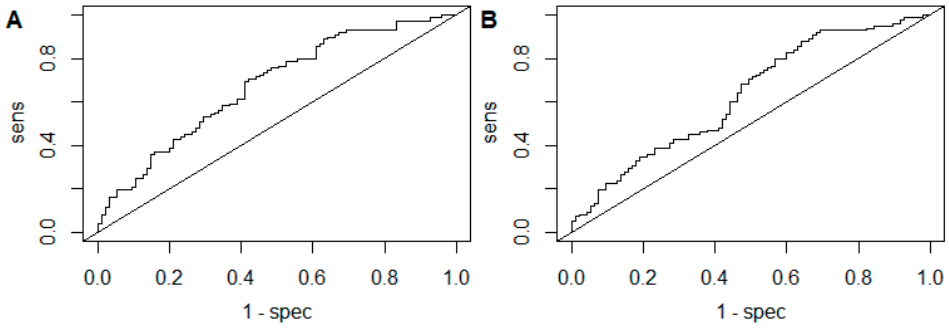


Figure S7. Receiver operator characteristics (ROC) curves for CSF with all amines. (A) Migraine with aura versus controls: area under the curve (AUC)=0.674. (B) Migraine without aura versus controls: area under the curve (AUC)=0.630, sens=sensitivity, spec=specificity.

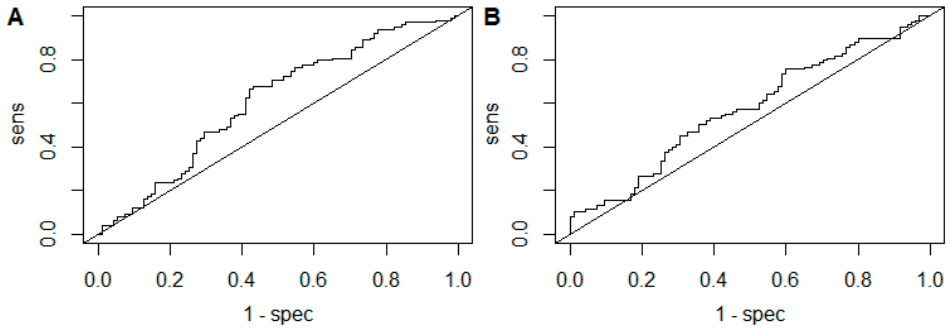


Figure S8. Receiver operator characteristics (ROC) curves for plasma with all amines. (A) Migraine with aura versus controls: area under the curve (AUC)=0.610. (B) Migraine without aura versus controls: area under the curve (AUC)=0.573, sens=sensitivity, spec=specificity.

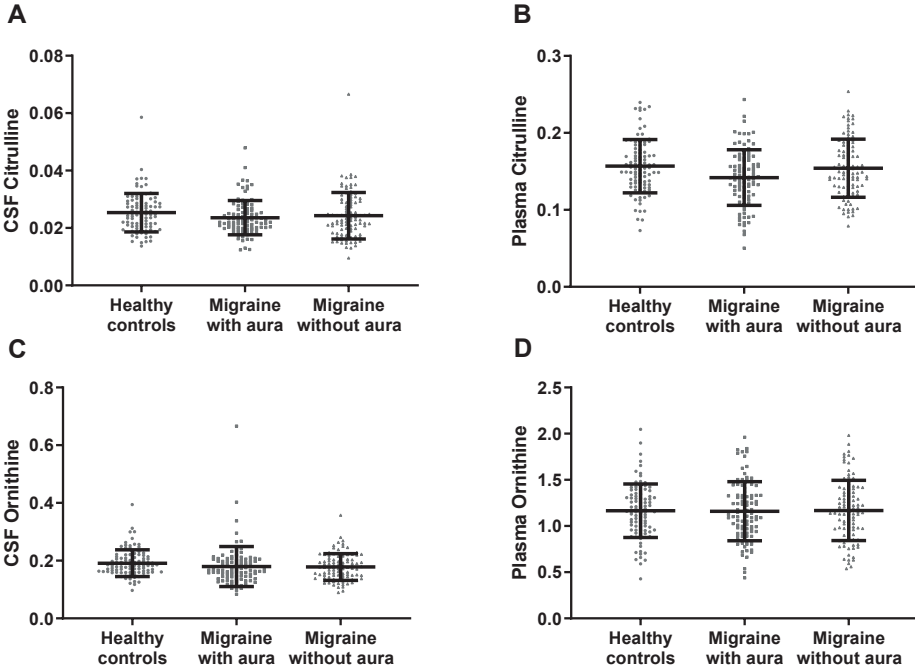


Figure S9. CSF and plasma Citrulline and Ornithine levels in participants with migraine and healthy controls. (A) Individual CSF Citrulline levels are plotted (dots) with group means \pm SD (bars). (B) Individual plasma Citrulline levels are plotted (dots) with group means \pm SD (bars). (C) Individual CSF Ornithine levels are plotted (dots) with group means \pm SD (bars). (D) Individual plasma Ornithine levels are plotted (dots) with group means \pm SD (bars). Data are adjusted for age.

